Future impacts of ozone driven damages on agricultural systems

Jon Sampedro[a,b,*], Stephanie Waldhoff[a], Dirk-Jan Van de Ven[b], Guillermo Pardo[b], Rita Van Dingenen[c], Iñaki Arto[b], Agustín del Prado[b] , Maria Jose Sanz[b]

[a] *Joint Global Change Research Institute, Pacific Northwest National Laboratory, 5825 University Research Court, Suite 3500, College Park, MD 20740, USA*
[b] *Basque Centre for Climate Change (BC3), Sede Building 1, 1st floor Scientific Campus of the University of the Basque Country. 48940 Leioa*
[c] *Joint Research Centre, Energy, Transport and Climate Directorate, Via Enrico Fermi 2749, 21027, Ispra (VA), Italy*

ABSTRACT

Current ozone (O_3) concentration levels entail significant damages in crop yields around the world. The reaction of the emitted precursors (mostly methane and nitrogen oxides) with solar radiation contribute to O_3 levels that exceed established thresholds for crop damage. This paper shows current and projected (up to 2080) relative yield losses (RYLs) driven by O_3 exposure for different crops and the associated economic damages applying dynamic crop production and prices that are calculated per region and period. We adjust future crop yields in the Global Change Assessment Model (GCAM) to reflect the RYLs and analyze the effects on agricultural markets. We find that the changes (generally reductions) in O_3 precursor emissions in a reference scenario would reduce the agricultural damages, compared to present, for most of the regions, with a few exceptions including India, where higher future O_3 concentrations have large negative impacts on crop yields. The annual economic impact of O_3 driven losses from 2010-2080 are, in billion US dollars at 2015 prices ($B), 5.0-6.0, 9.8-18.8, 6.7-10.6 and 10.4-12.5 for corn, soybeans, rice and wheat, respectively, with the large losses for wheat and soybeans driven by their comparatively high responses to O_3. When O_3 effects are explicitly modelled as exogenous yield shocks in future periods, there is a direct impact in future agricultural markets. Therefore, the aggregated net present value (NPV) of crop production would be reduced around by $90.8B at a global level. However, these changes are not distributed evenly across regions, and the net present market value of the crops would increase by up to $118.2B (India) or decrease by up to $59.2B (China).

Keywords: ozone, yield damages, agricultural systems, integrated assessment

JEL codes: Q11, Q21, Q51

*Corresponding author: Jon Sampedro. Joint Global Change Research Institute, Pacific Northwest National Laboratory, 5825 University Research Court, Suite 3500, College Park, MD 20740, USA
e-mail: jon.sampedro@pnnl.gov

1 Introduction

Tropospheric ozone (O_3) is the most hazardous pollutant for crop yields (Emberson et al., 2018). When crops are exposed to high O_3 concentration levels, it penetrates through the stomata during plant gas exchange and, as a strong oxidant, it induces several harmful effects, such as visible foliar injuries (necrosis and chlorosis), reduced photosynthesis, gene alteration, and a reduction in yields (Avnery et al., 2011a; Emberson et al., 2018). While other variables, such as temperature, precipitation or carbon fertilization effect (CFE) may affect crop yields, exposure to O_3 has the largest effect within expected environmental changes (Shindell, 2016) and is consistently negative, while impacts associated with changing climate may have negative or positive impacts, depending on crop, location, and climate projection. Consequently, the O_3-related decrease in crop yields would increase pressures on several measures associated with food security (Long et al., 2005; Mills et al., 2011). Recent studies have shown that different crop varieties have different response to O_3 exposure in some crops such as winter wheat (Biswas et al., 2009) or soybeans (Osborne et al., 2016), which could make O_3-related food security impacts uncertain.

The main driver for O_3 formation is the reaction of the emitted precursors with solar radiation. Changes in meteorological conditions, such as temperature variations, would also significantly affect O_3 levels, as demonstrated in different studies (Coates et al., 2016; Cox and Chu, 1996). Prior literature has extensively analyzed the effect of both greenhouse gases (GHG), including methane (CH_4), and non-GHG air pollutants such as nitrogen oxides (NO_X), carbon monoxide (CO), and non-Methane Volatile Organic Compounds (NMVOC) on O_3 formation (Burney and Ramanathan, 2014). However, O_3 formation is also partially determined by natural precursors such as biogenic nitrogen oxides missions (lightening and soils), wildfires or biogenic volatile compounds (BVOCs) emissions (Cooper et al., 2014).

In terms of historical O_3 concentration levels, Griffiths et al., (2020) in the framework of the Phase 6 of the Coupled Model Intercomparison Project (CMIP6), shows that current O_3 levels have increased around 40% compared to preindustrial levels (1850). This finding is consistent with the historical trends presented by Young et al., (2013) in the Atmospheric Chemistry and Climate Model Intercomparison Project (ACCMIP). O_3 concentrations have decreased in developed countries in recent years (Cooper et al., 2014), while other regions, such as developing Asia, have substantially increased their O_3 levels (Chang et al., 2017). Even though several regions have established different O_3-control measures[1], the increase of global methane emissions[2] and the increment in natural wildfires would increase O_3 levels, so more stringent control policies may be required (Lin et al., 2017).

[1] In addition to individual countries, several international agencies, namely the World Health Organization (WHO) or the Environmental Protection Agency (EPA), have established different targets and measures for controlling O_3 concentration levels (Ainsworth et al., 2012).

[2] Because of the long equilibration time, changes in O_3 concentrations attributable to variations in methane emissions are independent of the location of those methane emissions (Van Dingenen et al., 2018a).

Several studies predict that the reduction of precursor emissions coming from implemented climate policies would result in a significant decrease of O_3 concentration levels (Dentener et al., 2005; Sicard et al., 2017). Furthermore, the atmospheric transportation of those species entails significant inter-regional effects (Fiore et al., 2009). The individual effects of O_3 precursors vary[3] and, due to these differences, some studies demonstrate that mitigation actions for NO_X or CH_4 would be the most effective ones in order to reduce O_3 concentration levels (Shindell et al., 2019; West et al., 2007), even though in VOC-limited conditions, reducing NOx can lead to increased O_3 concentrations (Fiore et al., 1998). In addition, some studies have analyzed the effectiveness of the improvement of agricultural practices as a measure to reduce O_3 damages (Teixeira et al., 2011). They found that modifying crop calendars or crop varieties could be an adequate action for some concrete crops in some concrete regions, but there would not be a significant effect at a global level.

Different studies have analyzed current O_3-related crop damages using exposure-response functions (ERF) (Avnery et al., 2011a, 2011b; Feng et al., 2019; Ghosh et al., 2018; Van Dingenen et al., 2009; Vandyck et al., 2018). According to their results, focusing on year 2000, soybeans and wheat are the most O_3 sensitive crops, with global yield losses ranging from 6% to 16% and from 4% to 15%, respectively, depending on the region. Rice and corn would be less affected, as their potential crop damages in 2000 would account for 3-4% and 2.5-5.5%, respectively. Wang and Mauzerall (2004) showed that some Asian regions (China, Japan and South Korea), would have significantly higher O_3 damages on crops. According to this study, in those regions in 1990, the O_3 driven yield losses ranged from 1% to 9% for wheat, corn and rice, while, for soybeans, the damages would range between 23% and 27%. Those losses would increase for 2020, when wheat, corn and rice reduce their yield by 2 to 16%, and soybeans by 28% to 35%. Some literature estimates future O_3 effects on crops. Van Dingenen et al. (2009) show the potential crop losses for 2030, following the "current legislation" scenario (CLE)[4]. These authors use the TM5 Fast Scenario Screening Tool (TM5-FASST) air quality model to show that relative yield losses will be significantly larger in 2030, mostly for wheat and rice. The additional yield losses for these crops will amount 2-6% and 1-6% respectively, due to the increase on future O_3 concentration levels. In this line, Chuwah et al. (2015) combines an integrated assessment model (IMAGE) with TM5-FASST, and they report that crop losses might reach up to 20% in 2050. In addition, they show that by implementing stringent climate policies (Representative Concentration Pathway (RCP) 2.6), those yield losses would be significantly limited, not exceeding 10% in any region.

The studies mentioned do estimate current or future agricultural damages based on different methodologies. However, to our knowledge, this study is the first study estimating economic impacts associated to crop exposure to O_3 using temporal and regionally dynamic agricultural production and price estimations. For that purpose, we

[3] O_3 concentrations respond linearly to reductions in CH_4, CO and NMVOC emissions (Fiore et al., 2009, 2008), but the O_3 decrease would be greater (non-linear) with NO_X reductions (Wu et al., 2009).
[4] Details of the scenario can be found in Stohl et al., 2015

have developed and applied an innovative approach that subsequently connects an integrated assessment model (Global Change Assessment Model, GCAM) with an air quality tool (TM5-Fast Scenario Screening Tool, TM5-FASST), explained in detail in the following section. In addition, this integrated framework can be used to observe the relative importance of incorporating O_3 damages into scenario analysis. Another innovative aspect of this study is that it compares the net present value of crop losses by comparing a scenario without O_3 related crop damages with a similar scenario where O_3 damages are exogenously set as yield reductions. This is an important factor since projected reductions in yield productivity would alter the production of each commodity both globally and regionally due to changes in comparative advantage across regions. These changes in production levels and location of production consequently affect future crop prices. Moreover, crop demand is affected by different factors and does not directly respond to changes in yield productivity. These effects are captured by using an integrated assessment model (GCAM).

2 Materials and Methods

This study uses GCAM and TM5-FASST to assess the future impacts of O_3 driven damages on agricultural systems. GCAM is an integrated assessment model developed by the Joint Global Change Research Institute, which captures the dynamics of the socioeconomic, energy, land-use and climate systems. It tracks a wide variety of pollutants[5], for each period, region and sector, with internally consistent estimates of future O_3 precursors. The model divides the world in 32 regions and runs in 5-year time steps from 1990 to 2100[6].

In this study GCAM 4.4 is used with regionally differentiated agricultural markets that track gross imports and exports, and food consumption driven by prices and demand for staple and non-staple commodities[7], as the response of consumers to changes in prices and income are less elastic for staple crops than for non-staple crops. To meet global demand for agricultural products, farmers in different Agro-Ecological Zones (AEZs) (Monfreda et al., 2009) of each region compete on prices for their share in the regional market, and subsequently, regional markets compete with each other for their share in the global market for agricultural commodities. The competition between domestic and imported commodities are on the consumer side, following GCAM logit structure (Clarke

[5] It reports both GHGs and non-GHG air pollutants such as carbon dioxide (CO_2), methane (CH_4), nitrogen dioxide (N_2O), sulfur dioxide (SO_2), carbon monoxide (CO), nitrogen oxides (NOx), non-methane volatile organic compounds (NMVOC), ammonia (NH_3), black carbon (BC) or organic carbon (OC).

[6] For detailed information, see online documentation: https://github.com/JGCRI/gcam-doc/tree/gh-pages/v4.4

[7] Staple crops in GCAM are differentiated into five grains and roots/tubers commodities (corn, rice, wheat, other grain, roots/tubers). Non-staple foods consist of other crops (miscellaneous crops, oil crops, palm fruit, sugar crops) and animal products (dairy, beef, poultry, sheep/goat, other meat/fish). See table S2 in the SI for a full list of crop commodities used in GCAM.

and Edmonds, 1993), while the producer receives the same price for both domestic and export production.

Economic land use decisions in GCAM are based on a logit model of sharing (McFadden, 1973) based on relative inherent profitability of using land for competing purposes. The interpretation of this sharing system in GCAM is that there is a distribution of profit behind each competing land use within a region, rather than a single point value. Each competing land use option has a potential average profit over its entire distribution. The share of land allocated to any given use is based on the probability that that use has the highest profit among the competing uses (Wise et al., 2014; Zhao et al., 2020). The relative potential average profits are used in the logit formulation, where an option with a higher average profit will get a higher share than one with a lower average profit. The profit rate is the difference between the market price of the commodity and the production costs, which depend on land rent, fertilizer costs, other non-land costs and the crop yield. Crop yields in the base year (2010) are taken from FAO (2013) data and are calibrated for each of the AEZs within each of the 32 regions. For the estimation of future yields by region and AEZ, GCAM uses FAO projections through 2050 and, with the exception of fodder and fiber crops, yields for all crops in all regions are assumed to increase, but at decreasing rate, through 2100[8] (Bond-Lamberty et al., 2019).

The future path of O_3 precursor emissions reported by GCAM[9] is fed into the TM5-FASST model. TM5-FASST is an air quality source receptor model that, using atmospheric and meteorological information[10], transforms those precursors into region or grid (1ºx1º) level $PM_{2.5}$ and O_3 concentrations. Based on that information, the model estimates potential health and agricultural damages. Detailed information about TM5-FASST can be found in Van Dingenen et al. (2018b).

O_3-related agricultural damages are calculated for four representative crops, namely wheat, corn, rice and soybeans and they are estimated based on O_3-exposure indicators, exposure-response functions (ERFs), and spatially distributed crop production and growing seasons. In terms of O_3 indicators, TM5-FASST analyses crop exposures to O_3 based on two different metrics: “the accumulated daytime hourly O_3 concentration above a threshold of 40 ppb (AOT40)”, and the “seasonal mean daytime O_3 concentration (Mi)”, M7 for the 7-hour mean and M12 for the 12-hour mean (Van Dingenen et al., 2009) [11]. The calculations of the results are developed using AOT40, while the supplementary information (hereinafter SI) shows the results using the Mi indicator, as the metric used is a key factor for determining the results (Lefohn et al., 2018).

Following the definition of the UN Convention on Long-Range Transboundary Air Pollution (CLRTAP, 2017) and the Tropospheric Ozone Assessment Report (TOAR)

---

[8] http://jgcri.github.io/gcam-doc/aglu.html

[9] We have run a GCAM baseline scenario for this analysis, so we assume there is no climate policy or target established. The implications of the model assumptions are discussed in section 4.

[10] TM5-FASST is based on a single meteorological year (2001)

[11] M7 and M12 are indistinctly used as they are significantly correlated.

(Mills et al, 2018a), AOT40 is calculated as the sum of the differences between the hourly mean ozone concentrations and the specified threshold (40 ppb) for all daylight hours over a determined time horizon, which is three months in TM5-FASST. The units for AOT40 are parts per billion hours (ppb h). The reference height for O_3 concentrations in TM5-FASST is 30 meters, which is the mid-point of the TM5's lower layer grid box. O_3 is usually monitored at significantly lower altitudes (3 to 5 m), where concentration levels are lower due to deposition or other chemical processes. However, Van Dingenen et al., (2009) compares simulations at the reference height (30m) with monitored observation and demonstrates that crop metrics obtained from the grid box center reproduce the observations within their standard deviations. Therefore, the model does not apply a vertical profile correction factor, assuming a well-mixed 30m superficial layer.

AOT40 is calculated at grid level, based on O_3 hourly surface concentrations (1°x1°). These indicators are combined with growing season data in order to obtain gridded 3-monthly accumulated indices, which are the inputs for exposure-response functions used for estimating percentage relative yield losses (RYLs). Gridded crop data, including crop growing season and crop suitability index (based on average climate of 1961–1990), comes from the Global Agro-Ecological Zones V.3 database (GAEZ V.3). This data set provides gridded information on the crop-specific growth cycles, considering the number of days from crop emergence to full maturity. Growth cycles are determined optimally to obtain best possible yields for each crop. A detailed description on this data set is available online[12].

The exposure-response functions (ERFs) that TM5-FASST applies for estimating regional crop damages for wheat, corn, rice and soybeans at grid level (1°x1°), are based on a linear model[13], which is built from crop-response data from more than 700 studies, and is described in Mills et al., (2007). Then, RYLs, calculated at grid level, are weighted to region level by the crop production per grid cell, using the gridded crop production maps from GAEZ V.3.

To calculate the economic impacts, estimated relative crop losses (RYLs) for each region and period are multiplied by the agricultural production levels and market prices, obtained from GCAM for every region and period. Literature has demonstrated that applying a current price could result in significant underestimation of economic losses (Heck et al., 1987). This study overcomes that limitation as it is based on a dynamic integration of different models.

As the model is calibrated for 2010, the damages are included as yield shocks relative to that base year. Using regional agriculture production projections from GCAM combined with the RYLs from TM5-FASST, we estimate economic damages by multiplying the

[12] http://gaez.fao.org/Main.html
[13] While for AOT40 the ERFs are linear, for Mi, the ERFs follow a Weibull distribution (Wang and Mauzerall, 2004).

RYL by the projected production (Q) and price (P) levels for each crop, region, and period, as summarized in the following equation:

$$\text{Economic Damage}_{t,i,j} = \text{RYL}_{t,i,j} \times \text{P}_{t,i,j} \times \text{Q}_{t,i,j} \qquad (1)$$

where *t*, *i* and *j* represent the period, region and crop, respectively.

Finally, the obtained O_3 damage coefficients (per period and region) are re-set into GCAM, as exogenous yield shocks. So, we have compared the outcomes of a default GCAM baseline (no future changes in O_3 effects) with the scenario where we incorporate the estimated O_3-related yield changes per period and region. This innovative procedure makes it possible to see the impacts on agricultural systems by including the O_3 damages into future projections. For that purpose, we have calculated the difference of the net present value (NPV) of crop production for the two scenarios, as noted in the following equation:

$$\Delta\text{NPV}_{i,j} = \text{NPV}_{i,j}(\text{scen}) - \text{NPV}_{i,j}(\text{base})$$

$$\Delta\text{NPV}_{i,j} = \sum_t \frac{\text{P}_{t,i,j}(\text{scen}) \times \text{Q}_{t,i,j,}\,(\text{scen}) - \text{P}_{t,i,j}(\text{base}) \times \text{Q}_{t,i,j}(\text{base})}{(1+r)^t} \qquad (2)$$

where *P* and *Q* are the crop price and the production, and *t*, *i* and *j* represent the period, region and commodity, respectively. In this study, the discount rate (r) is 3% and the base year is 2010 for NPV calculation.

In a next step, we applied an index-decomposition analysis, following the Logarithmic Mean Divisia Index 1 method (Ang, 2004; Arto et al., 2009), in order to identify which are the factors that have the largest effects on the market value variation by crop. Table 1 lists the factors analyzed; detailed documentation on the decomposition analysis can be found in section 4 of the SI.

Factor	Description
Price effect (ΔP)	Changes in NPV of crop production due to changes in prices
Yield effect (ΔY)	Changes in NPV of crop production due to direct changes in yields
Land share effect (ΔsL)	Changes in NPV of crop production due to changes in land shares of different crops
Total land use effect (ΔLU)	Changes in NPV of crop production due to variations of total land dedicated to crop production

Table 1: Factors contributing to the change in the Net Present Value (NPV) of crop production between two scenarios.

TM5-FASST model only calculates damage coefficients for four crops (wheat, corn, rice and soybeans), so omitting the impacts on other crops would distort the RYLs across crops and the market equilibria. In order to avoid that inconsistency, we have expanded the losses to all the crops, using a crop mapping based on their carbon fixation pathway. C3 and C4 plant species present differences in stomatal conductance and transpiration rates, which determine their sensitivity to O_3 damage (Ainsworth, 2017; Knapp, 1993) Based on this criterion, the corn damage coefficient is applied to C4 classified commodities, while for C3 crops, the average damage of rice and wheat (or rice, wheat and soybean) is considered depending on the crop type classification (Table S3)[14].

3 Results

Figure 1 shows CH_4 and NO_X emissions per region and period, as they are the most significant pollutants for O_3 formation (Shindell et al., 2019; West et al., 2007). The emissions of other O_3 precursors such as NMVOCs[15] can be found in the SI. Note that the results are presented for 32 GCAM regions. The SI details the country to region mapping (table S1).

[14] This average includes damage coefficient from soybean for those crop groups that include legumes (f.e. MiscCrop).

[15] The model does not include CO-O_3 source-receptors, so O_3 will not be affected by changes in CO emissions

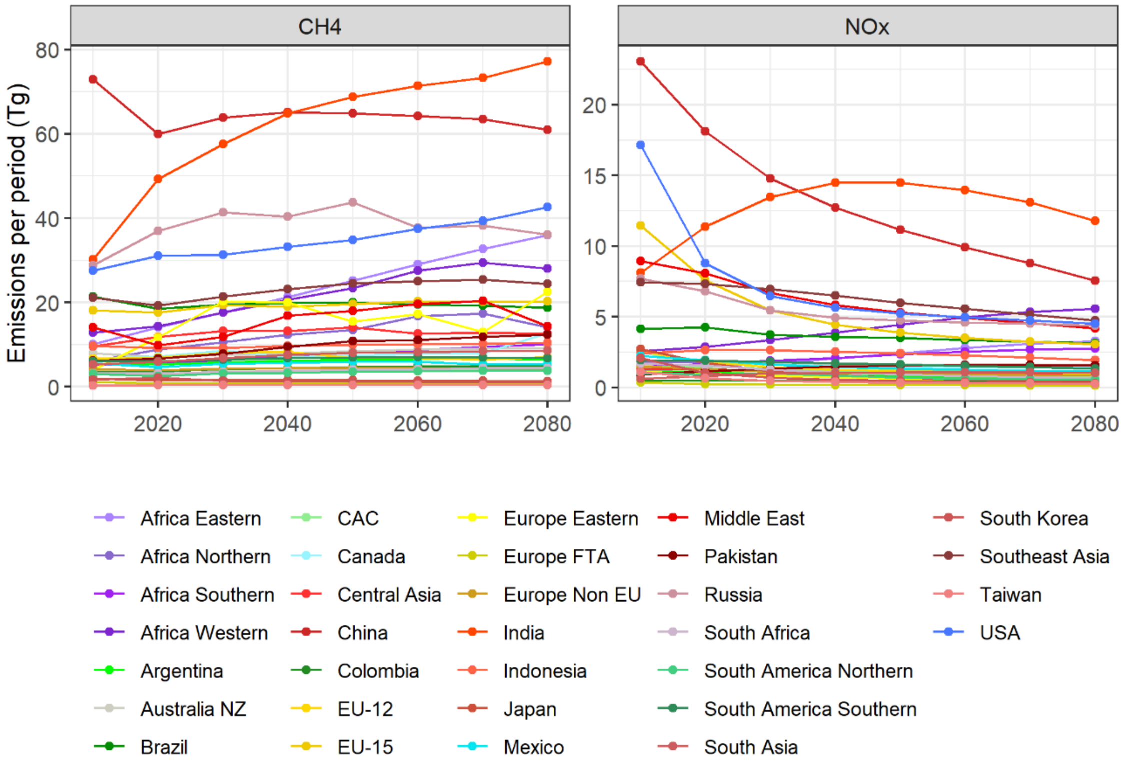

Figure 1: O_3 main precursor emissions (CH_4 and NO_X) per region and period (Tg). Simulations have been done with GCAM.

In absolute terms, China, India and USA (and Russia, for CH_4) have the largest emissions for both CH_4 and NO_X. However, future CH_4 and NO_X emission pathways have different trends. Figure 1 shows that emissions of CH_4, with no climate policy established, would increase in almost all the regions, while NO_X emissions would be flat or decrease all around the world. The reason is that GCAM implicitly incorporates future measures against air pollutants, based on planned emission control policies or future technological developments related to income increases, which, despite the uncertainties, would better estimate future emissions based on historical observations (Smith et al., 2005). These emission pathways result in different O_3 levels for every period and region. Figure 2 shows the gridded annual averaged O_3 levels for the medium term (2050). For short (2030) and long (2080) term levels, see the SI.

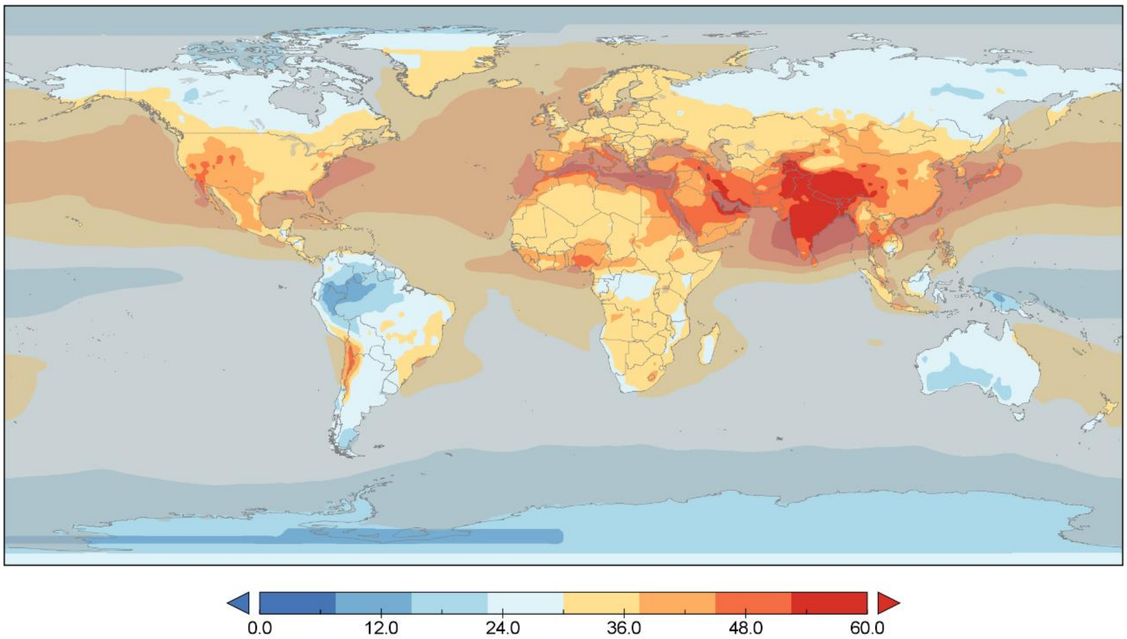

Figure 2: Annual average O_3 (ppb) in 2050. Emissions of precursors are simulated with GCAM and these are fed into TM5-FASST for estimating O_3 concentration levels.

Figure 2 shows two primary observations around O_3 distribution. First, the highest O_3 levels are formed around the equator. This happens because regions that are closer to the equator belt experience the largest solar irradiance and O_3 is formed when its precursors react with solar radiation. The map also shows the correlation between regional precursor emissions and O_3 concentration levels. Regions such as India, China or USA, which are the largest emitters of precursors (see Figure 1), have the highest O_3 levels[16].

[16] Short (2030) and long (2050) terms show similar trends on O_3, as can be seen in the SI.

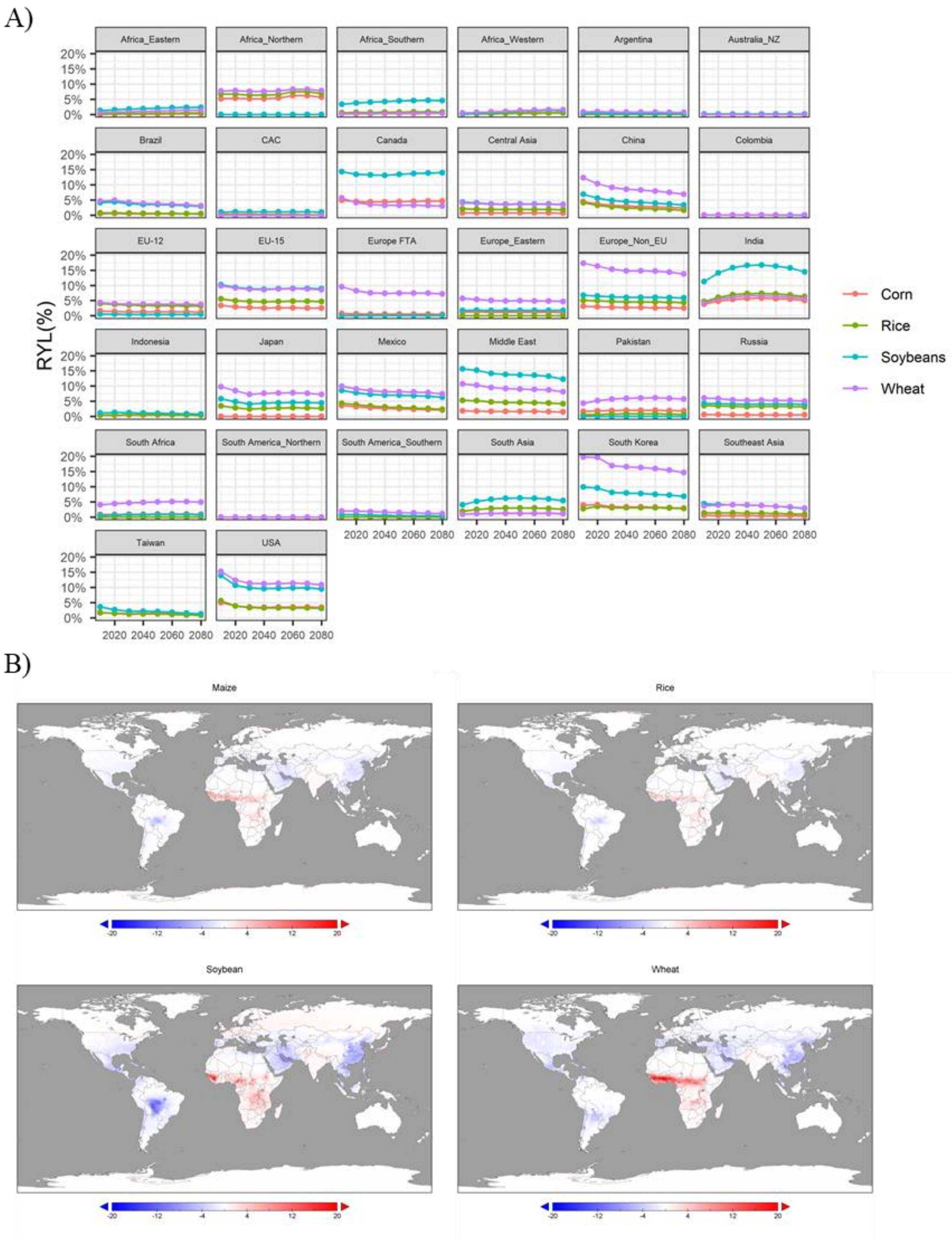

Figure 3: A) Relative Yield Losses (RYLs) related to O_3 exposure per period, crop and region (%). B) Gridded percentage difference in RYLs in 2080 compared to RYLs in 2020. Note that values in red (blue) indicate that there has been a decrease (improvement) in yield productivity. Emissions of precursors are simulated with GCAM and these are fed into TM5-FASST for estimating O_3 concentration levels and the subsequent RYLs based on exposure-response functions (ERFs).

The resulting yield losses due to these O_3 concentration levels for the mentioned crops (corn, rice, wheat and soybeans) are summarized in Figure 3. This figure shows that corn and rice crops are less affected by O_3 than wheat[17] and soybeans. The regions where corn suffers the largest yield losses during the analyzed time horizon (2020-2080) are Northern Africa (5-6%), India (4-6%), Canada (4-5%), USA (3-5%) and China (2.5-4.5%). Similar trends can be found for rice, as the most significant RYLs are in Northern Africa (6-7.5%) and India (5-7.5%). Wheat damages are relatively larger, accounting for 15-19% in South Korea, 14-17% in Europe Non-EU[18], 10-15% in USA, 7-12% in China, 8-10% in EU-15 and Middle East and 7.5-8.5% in Northern Africa. Likewise, soybeans suffer substantial RYLs in this time horizon, with largest effects in India (11-17%), Canada (13-14%), Middle East (12-15%) and USA (9-13%).

Figure 3B also demonstrates that most of the regions have decreasing RYLs for each crop up to 2080 compared to current damages, due to the reduction of future O_3 concentration levels. However, some regions show larger RYLs over time, driven by significant increases in some precursors. For example, in India, future crop damages would increase with respect to current levels. In 2050, the relative increments (with respect to the base year) range from 47% (soybeans) to 56% (rice). This is driven primarily by the substantial increase in CH_4 emissions through 2050[19] ,which more than double with respect to 2010 (127%) (see Figure 1). This effect is softened in 2080, as indicated in the gridded maps. The SI includes a detailed table of the RYL per region, crop and period applying both AOT40 and Mi metrics (Table S4). The estimated yield losses have an associated economic impact (see eq 1), as presented in Figure 4[20].

[17] While wheat damages during the study are calculated using "total wheat" values, the SI (figure S3) includes RYL coefficients for spring and winter wheat.

[18] This region includes, Albania, Bosnia-Herzegovina, Croatia, Macedonia and Turkey

[19] GCAM estimates that the large population growth in India would entail an increase in the demand for dairy products (from 95 Mt in 2010 to 445 Mt in 2050), which would subsequently increase CH_4 emissions

[20] In GCAM, soybeans are included the oilcrop category. Economic damages have therefore been estimated for the whole category. See Table S2 in the SI for a full list of commodities included in this category.

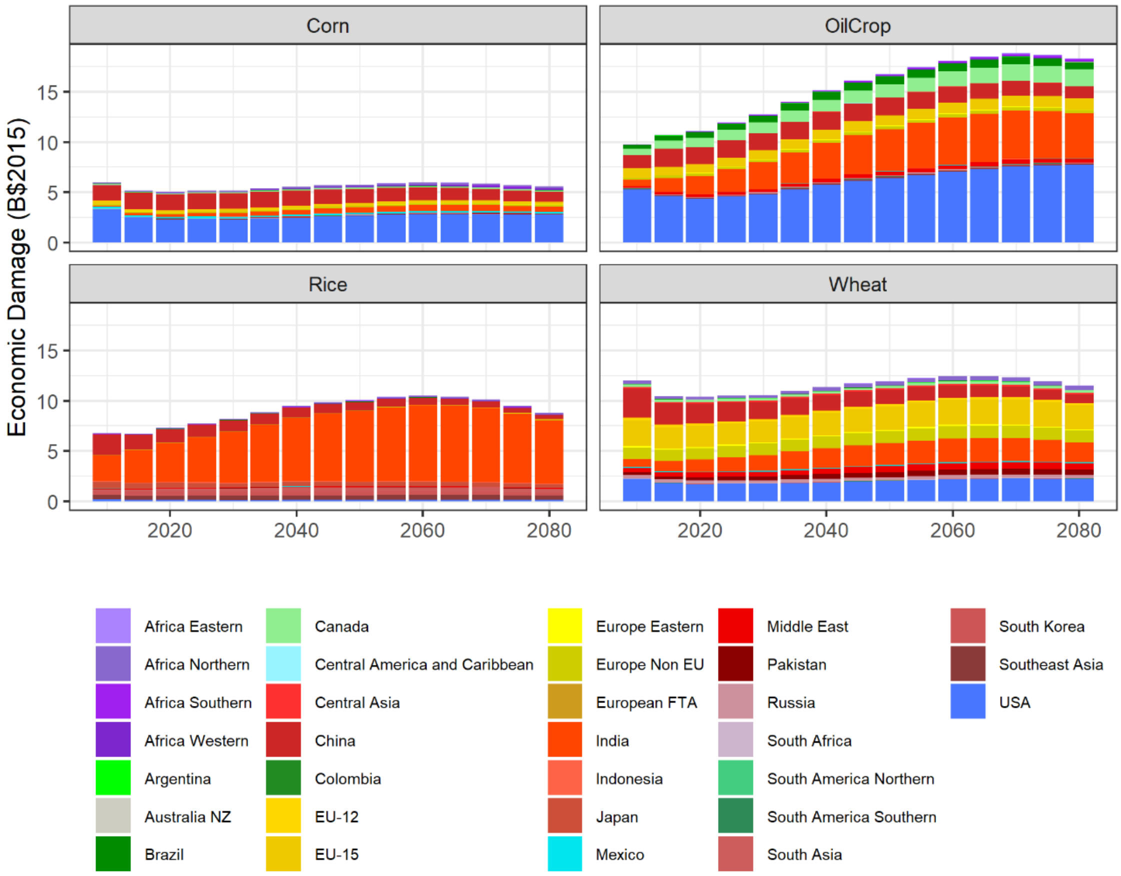

Figure 4: Economic damage driven by O_3 exposure per region, period and crop in billion \$ at 2015 prices (B\$(2015)). Emissions of precursors are simulated with GCAM and these are fed into TM5-FASST for estimating O_3 concentration levels and the subsequent RYLs based on exposure-response functions (ERFs). RYLs are then multiplied by region, crop and period-based prices and production levels obtained from GCAM simulations.

Figure 4 shows that corn driven economic losses decrease in the short term, and, then, they remain relatively unaltered, ranging from \$5.0 to 6.0 billion at 2015 prices (\$B). USA, which is the largest corn producer (33-38%, over time), bears the majority of damages, accounting for 44-55% of global corn damages, depending on the period. China, which produces between 18% and 23% of the corn, also experiences a large share of the damages (18-31%). Oilcrops, the category that includes soybeans, show a large increase in economic damages, from \$9.8B in 2010 to \$18.3B in 2080. The increase in damages in this crop is driven largely by increasing production volumes, mostly in USA, which is the largest oilcrop producer (18-22% of total production). The increase in oilcrop production is driven by an increase on demand for feed[21] and biodiesel production. In regional terms, USA has the largest damage (38-54%) followed up by India, which has only 7% of the economic damages in 2010, but 24% of global oilcrop damages by 2080. Economic damages of rice also increase during most of the 21st century (from \$6.8B in

[21] Meat production increases around 75% (818 Mt) up to 2050 at a global level. Consequently, the increase in feed production entails a significant increment in oilcrop (soybean cake) demand, accounting for 61 Mt (34%).

2010 to $10.1B in 2070). China, India and Southeast Asia are the largest producers; however, economic damages in Southeast Asia are small due to relatively lower O_3 concentration levels. Therefore, India (in the long term) and China experience most of the damages. These regions represent between 37-72% and 5-30% of the total rice damages, respectively. Global production changes during the analyzed period are smaller than 10%, which means that, as opposed to oilcrops, the increase of economic damages in rice production would be directly driven by higher O_3 concentration levels in future periods. Finally, the figure shows that economic damages of wheat are fairly constant, ranging from $10.4B to $12.5B during the analyzed time period. Although the regional allocation of the damages varies through the time horizon, the costs are principally borne by four of the larger producers: China, EU-15, India, and USA. In 2020, China experiences the largest damages (19-24% of the global wheat damages), followed by EU-15 (20-21%), USA (16-18%), and India (7-12%). However, in the long term (2080), damages in China (7%) drop drastically while they increase in India (17%). In 2080, the largest impacts are located in EU-15, USA and India, representing the 21%, 19% and 17% of the total wheat damages, respectively. In order to analyze the O_3 effects on agricultural markets, we evaluate the O_3 driven variations on the cumulative (2010-2080) NPV of crop production. Table 2 summarizes the decomposed (and total) effects for different regions (see section 2).

Region	ΔP	ΔY	ΔsL	ΔLU	ΔNPV
Africa Eastern	-2.75	-4.38	2.02	-3.27	**-8.40**
Africa Northern	-6.95	-0.42	-0.79	-3.60	**-11.77**
Africa Southern	-0.54	-1.47	0.73	-2.36	**-3.65**
Africa Western	2.09	-14.29	6.35	-2.63	**-8.49**
Argentina	-11.38	0.17	-2.45	-6.69	**-20.36**
Australia NZ	-3.20	-0.67	0.77	-5.66	**-8.76**
Brazil	-9.10	5.76	1.68	-7.24	**-8.91**
Canada	-8.06	8.62	2.07	-5.05	**-2.41**
Central America and Caribbean	-2.18	0.18	0.29	-2.44	**-4.16**
Central Asia	-2.96	1.81	0.74	-2.48	**-2.89**
China	-178.19	200.04	4.92	-85.95	**-59.19**
Colombia	-0.62	0.02	0.40	-1.53	**-1.73**
EU-12	-11.49	4.87	-3.07	-7.02	**-16.70**
EU-15	-73.76	59.90	3.24	-37.75	**-48.40**
Europe Eastern	-6.93	3.09	-0.43	-3.18	**-7.46**
Europe Non-EU	-31.71	35.49	4.12	-11.28	**-3.38**
European Free Trade Association	-1.11	1.33	0.26	-0.44	**0.04**
India	215.30	-114.89	-9.87	27.75	**118.19**
Indonesia	-2.74	0.17	0.09	-1.02	**-3.50**
Japan	-8.08	6.57	0.18	-6.86	**-8.20**
Mexico	-13.14	14.70	2.92	-6.77	**-2.27**
Middle East	-21.74	20.79	2.01	-7.26	**-6.19**
Pakistan	1.24	-5.90	-1.73	-0.15	**-6.54**
Russia	-6.07	3.88	-0.62	-6.69	**-9.50**
South Africa	-0.74	-0.92	-0.79	-1.32	**-3.78**
South America Northern	-0.18	0.01	0.36	-0.79	**-0.60**
South America Southern	-3.98	1.29	-0.93	-4.46	**-8.08**
South Asia	1.65	-4.44	-0.74	0.10	**-3.44**
South Korea	-0.34	-1.69	0.22	-1.11	**-2.91**
Southeast Asia	-12.22	5.95	2.23	-7.21	**-11.25**
USA	-111.47	172.04	23.82	-10.55	**73.89**
TOTAL	**-311.32**	**397.59**	**37.99**	**-214.95**	**-90.80**

Table 2: Contribution of different factors to the cumulative (2010 - 2080) variations in the net present value (NPV) of crop production per region in billion $ at 2015 prices. The four factors are Price effect (ΔP), Yield effect (ΔY), Land share effect (ΔsL), and Total land use effect (ΔLU) (see Table 1). The last column (ΔNPV) shows the total change on the NPV of crop production aggregated per region, while the last row (TOT), shows the aggregation of each decomposed effect. Results are based on the combined application of GCAM and TM5-FASST.

Table 2 shows that in cumulative terms (2010-2080), the total NPV of crop production would be reduced by $90.8B$ at a global level. Productivity improvements driven by future O_3 reductions increase the output of the land and, therefore, for satisfying a determined demand, total land dedicated to crops decreases accordingly. So, these results entail positive effects to the consumer side (lower prices), while negative to the producer side (reduction in commercialized farmland[22]).

Regarding regional distribution, absolute changes in the NPV of crop production are largely concentrated in four regions: China, EU-15, India and USA, although some other regions such as Argentina, EU-12 or Southeast Asia also present significant variations. As shown in Figure 3, future increase in O_3 concentrations in India (and in some other regions such as Western Africa or South Asia) would reduce yield productivity (-$114.9B), so, although there would be more land dedicated to agriculture, commodity prices would subsequently increase ($215.3B), which could generate food insecurity and/or land use related hazards in these regions. On the other side, China and EU-15 (and most of the regions, with smaller impacts), are expected to reduce their future O_3 concentration levels, resulting in future improvements in yield productivity ($200.1B and $59.9B$ respectively). Therefore, the subsequent reduction on commodity prices and the decrease of the land dedicated to agriculture reduces the NPV of crop production in $59.19B and $48.4B respectively. Finally, USA also benefits from significant yield productivity improvements driven by a projected decrease of O_3 concentration levels ($172.04B), so there is less land dedicated to agriculture and commodity prices decrease. However, these effects do not outweigh the production increase driven by yield improvements, so the NPV of crop production increases in $73.89B in this region. The reason is that USA is the largest producer of corn, oilcrop, and wheat[23], and the increase in production driven by productivity improvements would increase global demand for biofuels, softening the price effect significantly.

4 Discussion

The application of the presented integrated methodology allows us to capture the interactions between the economic dynamics, emissions, atmospheric conditions and agricultural production. Therefore, the obtained results are directly related to the socioeconomic, environmental or land-use assumptions taken for future scenario projections. For example, current and future regional emission factors, food, and non-food demands for different crops, or population and GDP growth rates affect both global and regional results. Even though all future modelling projections have an inherent uncertainty, the models used in this study are well-accepted and have been extensively used by the scientific community. GCAM has been under development for more than 30 years and it has been applied in several multi-model and multi-sectoral analysis, including scenarios for the IPCC (Thomson et al., 2011) and the Shared Socioeconomic Pathways (Calvin et al., 2017). There is a large amount of peer reviewed studies using GCAM[24]. It has been coupled with different models or tools with different focus and is an important tool for the scientific community. Likewise, TM5-FASST has been widely used by

[22] This will have direct implications in CO_2 land use change (LULUCF) emissions, which are not considered in this study.
[23] EU-15, USA and India are the larger wheat producers, depending on the period.
[24] http://www.globalchange.umd.edu/publications/

different institutions (WB and ICCI, 2013; OECD, 2016) and in several peer reviewed scientific articles[25]. Additionally, the model documentation paper (Van Dingenen et al., 2018b) develops a detailed validation of TM5-FASST against a full global atmospheric chemistry transport model (TM5). The study shows that TM5-FASST replicates the atmospheric model in terms of additivity and linearity for both current values and future scenarios.

We have compared our results with other studies where ERFs are applied for estimating RYLs and/or economic damages. In year 2000, economic damages associated to O_3-related crop losses would account for \$10-26B according to the mentioned studies. We estimate that economic losses for 2010 (first year of analysis) represent around \$34B. Although we identify similar trends in some regions and for some crops, trends in terms of agricultural damages for several other crops diverge because regional land use, crop production levels, and crop demands are endogenous in GCAM, which allows for varying responses in regional production and consumption. In terms of future projections, results are not directly comparable since there are significant differences between the models used, the scenario definition and assumptions regarding future development levels. However, we do find that changes in RYLs through 2030 are consistent with Van Dingenen et al., (2009), Chuwah et al., (2015), and Vandyck et al., (2018) varying across regions, with increases in South-Asia (India or Bangladesh) and decreases in Europe or China. Regarding economic damages, Avnery et al., (2011b) estimate that annual economic losses in 2030 would range from \$12-35B at a global level, depending on the scenario. According to our results, economic losses in 2030 would amount \$36B. We have compared our economic damages with different global and regional studies (Feng et al., 2019; Ghude et al., 2014; Holland et al., 2006; McGrath et al., 2015; Sharma et al., 2019), which is summarized in Table 3.

[25] A summary of some of these studies is presented in Van Dingenen et al., (2018b), S1.

Study	*Crops included*	*Year*	*Annual Economic losses ($B)*
Global			
Avnery et al., 2011a, 2011b	Maize, Soybeans, Wheat	2000 2030	11 - 18 12 - 35
Van Dingenen et al., 2009	Maize, Soybeans, Rice, Wheat	2000	14 - 26
Present study	Maize, Soybeans*, Rice, Wheat	2010 2030 2050 2080	34 36 44.5 44
China			
Avnery et al., 2011a, 2011b	Maize, Soybeans, Wheat	2000 2030	2.5 - 3.5 5 - 8.5
Feng et al., 2019	Rice, Wheat	2015	18.6
Van Dingenen et al., 2009	Maize, Soybeans, Rice, Wheat	2000	3-5.5
Wang and Mauzerall, 2004	Maize, Soybeans, Rice, Wheat	1990 2020	3.5 6.5
Present study	Maize, Soybeans, Rice, Wheat	2010 2030 2050 2080	7.8 6.1 5.4 3.5
European Union			
Holland et al., 2006	23 crops	2000 2020	8.4 5.6
Van Dingenen et al., 2009	Maize, Soybeans, Rice, Wheat	2000	0.8 - 1
Present study	Maize, Soybeans, Rice, Wheat	2010 2030 2050 2080	4.2 3.5 3.9 4
India			
Avnery et al., 2011a, 2011b	Maize, Soybeans, Wheat	2000 2030	1 - 4 1.5 – 8.5
Ghude et al., 2014	Soybeans, Rice and Wheat	2005	1.2
Sharma et al., 2019	Rice and Wheat	2015	6.5
Van Dingenen et al., 2009	Maize, Soybeans, Rice, Wheat	2000	2.8 – 6.1
Present study	Maize, Soybeans, Rice, Wheat	2010 2030 2050 2080	4.1 9.6 13.9 13.3
USA			
Avnery et al., 2011a, 2011b	Maize, Soybeans, Wheat	2000 2030	2.5 – 3.5 3.5 – 4.5
McGrath et al., 2015	Maize, Soybeans	1980 - 2011	9
Van Dingenen et al., 2009**	Maize, Soybeans, Rice, Wheat	2000	1.8 - 4
Present study	Maize, Soybeans, Rice, Wheat	2010 2030 2050 2080	11 8.9 11.2 12.8

*Present study estimates damages for oilcrops, which includes more than soybeans (see table S2 in the SI)
**Economic losses for North America

Table 3: Comparison of annual economic damages between this study and previous estimates in literature. Annual economic losses represent the sum of the damages for all crops included.

The use of ERFs is a well-accepted methodology for estimating RYLs that is adequate for scenario analysis within the context of an integrated modelling framework as presented in this work. However, this method has some limitations. ERFs are based on European and North American information, due to lack of data in other regions, potentially resulting in underestimation of the O_3 driven crop losses in Asian regions (Emberson et al., 2009).

Recent studies are focusing on regional and national data in order to more accurately estimate the O_3 impacts on crops in different regions outside of North America and Europe, such as China (Feng et al., 2017; Yi et al., 2020), India (Singh and Agrawal, 2017) or Africa (Hayes et al., 2019). The integrated modeling framework applied in this study analyses the entire world in a national scale, and it uses global inventories to calibrate and estimate current and future emissions of O_3 anthropogenic precursors. Even though different data sources report some regional differences in emissions of O_3 precursors[26], the model consistently estimates future emission trajectories. In the case of China, recent studies have estimated that NO_x emissions have decreased around 20% from 2013 to 2017 (Li et al., 2019; Zheng et al., 2018). According to GCAM simulations, the NO_x reduction in China from 2010 to 2020 would account for 21%.

In terms of sub-regional dynamics, TM5-FASST does not consider emission pattern changes within each country. In China, results show high O_3 levels around the Himalaya and the Tibetan Plateau, which is consistent with prior studies (Dentener et al., 2006; Moore and Semple, 2009). Recent studies estimate that O_3 levels in some cities in Eastern China would reach up to 70-100 ppb in 2017 (Chen et al., 2018; Li et al., 2019; Wang et al., 2017), while our estimates show smaller annual averaged concentration levels (50-70 ppb). However, TM5-FASST implicitly incorporates emission-concentration sensitivities, and the Figure S3 in the SI shows the relation between NO_x emissions and O_3 concentrations for China, measured as the monthly accumulated hourly O_3 above 40 ppb per kg emitted during daytime. The figure shows that Eastern China is by far the most sensitive region, especially in summer (June). Conversely, wintertime O_3 titration in the most polluted locations brings down O_3 on an annual basis[27], so the annually averaged values presented in Figure 2 would be significantly reduced in Eastern China. Nevertheless, if it turns out that future AOT40 levels in Eastern China are higher than estimated in this study, this will have consequences for overall damages in agricultural systems for China.

Regarding source-receptor coefficients, the SRCs used in ERFs are estimated based on present-day growing seasons (year 2000 in TM5-FASST). Future climate variations could impact growing seasons, which is an effect that is not captured with the application of these ERFs. Additionally, these studies do not capture vegetation dynamics, not considering physiological factors such as soil particularities, vapor pressure, transpiration, or evaporation (Emberson et al., 2018; Schauberger et al., 2019). This may potentially overestimate the O_3 impacts on crops in water scarce regions, while underestimating the effects in water abundant regions. This difference in the methodology may account for the smaller RYLs values for wheat in both China and India compared to

---

[26] For example, USA NOx emissions in the model are larger than the EPA-inventory emissions, as shown in Shi et al., (2017). The potential implications of the divergences in precursor emissions would have a direct effect on the variations on RYLs in that region, with the subsequent impacts on agricultural markets.

[27] In fact, for the winter months there is a negative correlation between NO_x emissions and O_3 production.

Schauberger et al., 2019; however, the RYLs for soybeans are notably larger when applying ERF models than when considering the whole vegetation system.

In addition, recent literature has shown that yield losses based on stomatal uptake or flux dose-response models would be more accurate, as it has been demonstrated that ozone effects are more greatly correlated with stomatal uptake than with ozone concentrations (Mills et al., 2018b, 2018c; Pleijel et al., 2007). Even though the methods used in this work differ to the mentioned studies there are some similar outcomes, as they show that wheat and soybeans are the most affected crops while rice and maize would be less impacted (Mills et al., 2018b). Moreover, Mills et al., (2018c) shows that currently, RYLs for wheat would represent around 6-10%, being USA and China the some of the most affected regions. These conclusions are similar to the results presented in this study.

Regarding the crop exposure to O_3, we identify that the applied AOT40 measure has some limitations. First, this metric omits O_3 concentration below 40 ppb which may have additional effects (Emberson et al., 2009)[28]. However, AOT40 is considered a robust exposure indicator and allows for result comparison with different studies[29]. In order to address this uncertainty and see the effect of the indicator on RYLs we have re-calculated the RYL coefficients by using Mi exposure indicator (table S4). The table shows that the differences in RYLs driven by the exposure metric would vary per region and crop but, in general, while corn and rice show more similar results, there are large divergences in wheat and, especially, soybean RYLs. Additionally, TM5-FASST only allows estimation of the RYLs for four crops, requiring extrapolation of the damages to other commodities based on their carbon fixation pathway (see section 2). Although there exist additional ERF functions for other crops (Mills et al., 2007), the structure of GCAM, which combines crops in aggregate commodities, does not allow to apply those individualized functions. This is planned to be explored in further research.

Finally, this work focuses exclusively on the O_3 impacts on crop yields. Future work is planned to explore the combined effects of O_3 and climate change impacts, due to changing temperature or precipitation, and carbon fertilization effects (Ainsworth et al., 2012; Guarin et al., 2019; Reilly et al., 2007; Tai et al., 2014). This combined approach could provide a more holistic perspective of the potential crop damages.

5 Conclusion

The study demonstrates that high O_3 concentration levels cause harmful impacts to crop yields all over the world. This conclusion is consistent across all the studies analyzed, even though they are based on substantially different models and methodologies. Results presented in this work indicate that there are significant crop losses and economic

[28] Additionally, the linearized source-receptor coefficients in TM5-FASST could over (or under) estimate the AOT40 change upon a precursor emission change, particularly in O_3 concentrations around the threshold (40 ppb) level (Van Dingenen et al., 2018b).

[29] It is also the measure used in semi-empirical models (Ren et al., 2007).

damages that could result in regional problems of food security and wealth losses. We believe that the magnitude of the results could encourage stakeholders and policymakers not only to take action for reducing harmful O_3 levels, but to consider O_3 as a relevant element in the design of future global change strategies. Additionally, we show that incorporating O_3 to scenario analysis is an important consideration as there are dynamic changes on the agricultural markets, such as variations in production and price levels that are directly attributable to O_3-driven yield losses. The outcomes in this study could boost modelling communities to incorporate O_3 effects in yields to individual scenario simulations or to model inter-comparison studies.

Acknowledgments

This research is supported by Basque Government through the BERC 2018-2021 and the Spanish Government through María de Maeztu excellence accreditation MDM-2017-0714. This research is also supported in part by US Environmental Protection Agency, under Interagency Agreement DW08992459801. Jon Sampedro, Dirk-Jan van de Ven and Iñaki Arto acknowledge financial support from the Ministry of the Economy and Competitiveness of Spain (RTI2018-099858-A-100 and RTI2018-093352-B-I00). Jon Sampedro acknowledge financial support from the Basque Government (PRE_2017_2_0139). Iñaki Arto acknowledge financial support from the European Union's Horizon 2020 research and innovation program under grant agreement no. 821105 (LOCOMOTION project). Agustin del Prado is financed by the programme Ramon y Cajal from the Spanish Ministry of Economy, Industry and Competitiveness (RYC-2017-22143). The views and opinions expressed are those of the authors, and do not necessarily represent the views or policies of the US EPA or other funding organizations.

References

Ainsworth, E.A., 2017. Understanding and improving global crop response to ozone pollution. Plant J. 90, 886–897.

Ainsworth, E.A., Yendrek, C.R., Sitch, S., Collins, W.J., Emberson, L.D., 2012. The effects of tropospheric ozone on net primary productivity and implications for climate change. Annu. Rev. Plant Biol. 63, 637–661.

Ang, B.W., 2004. Decomposition analysis for policymaking in energy:: which is the preferred method? Energy Policy 32, 1131–1139.

Arto, I., Gallastegui, C., Ansuategi, A., 2009. Accounting for early action in the European Union Emission Trading Scheme. Energy Policy 37, 3914–3924.

Avnery, S., Mauzerall, D.L., Liu, J., Horowitz, L.W., 2011a. Global crop yield reductions due to surface ozone exposure: 1. Year 2000 crop production losses and economic damage. Atmos. Environ. 45, 2284–2296. https://doi.org/10.1016/j.atmosenv.2010.11.045

Avnery, S., Mauzerall, D.L., Liu, J., Horowitz, L.W., 2011b. Global crop yield reductions due to surface ozone exposure: 2. Year 2030 potential crop production losses and

economic damage under two scenarios of O3 pollution. Atmos. Environ. 45, 2297–2309.
Biswas, D., Xu, H., Yang, J., Li, Y., Chen, S., Jiang, C., Li, W., Ma, K., Adhikary, S., Wang, X., 2009. Impacts of methods and sites of plant breeding on ozone sensitivity in winter wheat cultivars. Agric. Ecosyst. Environ. 134, 168–177.
Bond-Lamberty, B., Dorheim, K., Cui, R., Horowitz, R., Snyder, A., Calvin, K., Feng, L., Hoesly, R., Horing, J., Kyle, G.P., 2019. gcamdata: An R Package for Preparation, Synthesis, and Tracking of Input Data for the GCAM Integrated Human-Earth Systems Model. J. Open Res. Softw. 7.
Burney, J., Ramanathan, V., 2014. Recent climate and air pollution impacts on Indian agriculture. Proc. Natl. Acad. Sci. 111, 16319–16324. https://doi.org/10.1073/pnas.1317275111
Calvin, K., Bond-Lamberty, B., Clarke, L., Edmonds, J., Eom, J., Hartin, C., Kim, S., Kyle, P., Link, R., Moss, R., 2017. The SSP4: A world of deepening inequality. Glob. Environ. Change 42, 284–296.
Chang, K.-L., Petropavlovskikh, I., Cooper, O.R., Schultz, M.G., Wang, T., 2017. Regional trend analysis of surface ozone observations from monitoring networks in eastern North America, Europe and East Asia.
Chen, K., Fiore, A.M., Chen, R., Jiang, L., Jones, B., Schneider, A., Peters, A., Bi, J., Kan, H., Kinney, P.L., 2018. Future ozone-related acute excess mortality under climate and population change scenarios in China: A modeling study. PLoS Med. 15.
Chuwah, C., van Noije, T., van Vuuren, D.P., Stehfest, E., Hazeleger, W., 2015. Global impacts of surface ozone changes on crop yields and land use. Atmos. Environ. 106, 11–23. https://doi.org/10.1016/j.atmosenv.2015.01.062
Clarke, J.F., Edmonds, J.A., 1993. Modelling energy technologies in a competitive market. Energy Econ. 15, 123–129.
CLRTAP, 2017. Manual on methodologies and criteria for modelling and mapping critical loads and levels and air pollution effects, risks and trends. Chapter 3: Mapping critical levels for vegetation.
Coates, J., Mar, K.A., Ojha, N., Butler, T.M., 2016. The influence of temperature on ozone production under varying NO x conditions–a modelling study. Atmospheric Chem. Phys. 16, 11601–11615.
Cooper, O.R., Parrish, D., Ziemke, J., Cupeiro, M., Galbally, I., Gilge, S., Horowitz, L., Jensen, N., Lamarque, J.-F., Naik, V., 2014. Global distribution and trends of tropospheric ozone: An observation-based review.
Cox, W.M., Chu, S.-H., 1996. Assessment of interannual ozone variation in urban areas from a climatological perspective. Atmos. Environ. 30, 2615–2625.
Dentener, F., Stevenson, D., Cofala, J., Mechler, R., Amann, M., Bergamaschi, P., Raes, F., Derwent, R., 2005. The impact of air pollutant and methane emission controls on tropospheric ozone and radiative forcing: CTM calculations for the period 1990–2030. Atmos Chem Phys 25.
Dentener, F., Stevenson, D., Ellingsen, K. v, Van Noije, T., Schultz, M., Amann, M., Atherton, C., Bell, N., Bergmann, D., Bey, I., 2006. The global atmospheric environment for the next generation. Environ. Sci. Technol. 40, 3586–3594.
Emberson, L.D., Büker, P., Ashmore, M.R., Mills, G., Jackson, L.S., Agrawal, M., Atikuzzaman, M.D., Cinderby, S., Engardt, M., Jamir, C., Kobayashi, K., Oanh, N.T.K., Quadir, Q.F., Wahid, A., 2009. A comparison of North American and Asian exposure–response data for ozone effects on crop yields. Atmos. Environ. 43, 1945–1953. https://doi.org/10.1016/j.atmosenv.2009.01.005

Emberson, L.D., Pleijel, H., Ainsworth, E.A., van den Berg, M., Ren, W., Osborne, S., Mills, G., Pandey, D., Dentener, F., Büker, P., Ewert, F., Koeble, R., Van Dingenen, R., 2018. Ozone effects on crops and consideration in crop models. Eur. J. Agron. https://doi.org/10.1016/j.eja.2018.06.002

Feng, Z., De Marco, A., Anav, A., Gualtieri, M., Sicard, P., Tian, H., Fornasier, F., Tao, F., Guo, A., Paoletti, E., 2019. Economic losses due to ozone impacts on human health, forest productivity and crop yield across China. Environ. Int. 131, 104966.

Feng, Z., Tang, H., Kobayashi, K., 2017. Effects of Ozone on Crops in China, in: Air Pollution Impacts on Plants in East Asia. Springer, pp. 175–194.

Fiore, A.M., Dentener, F.J., Wild, O., Cuvelier, C., Schultz, M.G., Hess, P., Textor, C., Schulz, M., Doherty, R.M., Horowitz, L.W., MacKenzie, I.A., Sanderson, M.G., Shindell, D.T., Stevenson, D.S., Szopa, S., Van Dingenen, R., Zeng, G., Atherton, C., Bergmann, D., Bey, I., Carmichael, G., Collins, W.J., Duncan, B.N., Faluvegi, G., Folberth, G., Gauss, M., Gong, S., Hauglustaine, D., Holloway, T., Isaksen, I.S.A., Jacob, D.J., Jonson, J.E., Kaminski, J.W., Keating, T.J., Lupu, A., Marmer, E., Montanaro, V., Park, R.J., Pitari, G., Pringle, K.J., Pyle, J.A., Schroeder, S., Vivanco, M.G., Wind, P., Wojcik, G., Wu, S., Zuber, A., 2009. Multimodel estimates of intercontinental source-receptor relationships for ozone pollution. J. Geophys. Res. 114. https://doi.org/10.1029/2008JD010816

Fiore, A.M., Jacob, D.J., Logan, J.A., Yin, J.H., 1998. Long-term trends in ground level ozone over the contiguous United States, 1980–1995. J. Geophys. Res. Atmospheres 103, 1471–1480.

Fiore, A.M., West, J.J., Horowitz, L.W., Naik, V., Schwarzkopf, M.D., 2008. Characterizing the tropospheric ozone response to methane emission controls and the benefits to climate and air quality. J. Geophys. Res. Atmospheres 113.

Ghosh, A., Singh, A.A., Agrawal, M., Agrawal, S., 2018. Ozone Toxicity and Remediation in Crop Plants, in: Sustainable Agriculture Reviews 27. Springer, pp. 129–169.

Ghude, S.D., Jena, C., Chate, D., Beig, G., Pfister, G., Kumar, R., Ramanathan, V., 2014. Reductions in India's crop yield due to ozone. Geophys. Res. Lett. 41, 5685–5691.

Griffiths, P. T., Murray, L. T., Zeng, G., Archibald, A. T., Emmons, L. K., Galbally, I., Hassler, B., Horowitz, L. W., Keeble, J., Liu, J., Moeini, O., Naik, V., O'Connor, F. M., Shin, Y. M., Tarasick, D., Tilmes, S., Turnock, S. T., Wild, O., Young, P. J., and Zanis, P.: Tropospheric ozone in CMIP6 Simulations, Atmos. Chem. Phys. Discuss., https://doi.org/10.5194/acp-2019-1216, in review, 2020.

Guarin, J.R., Emberson, L., Simpson, D., Hernandez-Ochoa, I.M., Rowland, D., Asseng, S., 2019. Impacts of tropospheric ozone and climate change on Mexico wheat production. Clim. Change 155, 157–174.

Hayes, F., Sharps, K., Harmens, H., Roberts, I., Mills, G., 2019. Tropospheric ozone pollution reduces the yield of African crops. J. Agron. Crop Sci.

Holland, M., Kinghorn, S., Emberson, L., Cinderby, S., Ashmore, M., Mills, G., Harmens, H., 2006. Development of a framework for probabilistic assessment of the economic losses caused by ozone damage to crops in Europe.

Knapp, A.K., 1993. Gas Exchange Dynamics in C^ 3 and C^ 4 Grasses: Consequence of Differences in Stomatal Conductance. Ecology 74, 113–123.

Lefohn, A.S., Malley, C.S., Smith, L., Wells, B., Hazucha, M., Simon, H., Naik, V., Mills, G., Schultz, M.G., Paoletti, E., De Marco, A., Xu, X., Zhang, L., Wang, T., Neufeld, H.S., Musselman, R.C., Tarasick, D., Brauer, M., Feng, Z., Tang, H., Kobayashi, K., Sicard, P., Solberg, S., Gerosa, G., 2018. Tropospheric ozone assessment report: Global ozone metrics for climate change, human health, and crop/ecosystem research. Elem Sci Anth 6, 28. https://doi.org/10.1525/elementa.279

Li, K., Jacob, D.J., Liao, H., Shen, L., Zhang, Q., Bates, K.H., 2019. Anthropogenic drivers of 2013–2017 trends in summer surface ozone in China. Proc. Natl. Acad. Sci. 116, 422–427.

Lin, M., Horowitz, L.W., Payton, R., Fiore, A.M., Tonnesen, G., 2017. US surface ozone trends and extremes from 1980 to 2014: quantifying the roles of rising Asian emissions, domestic controls, wildfires, and climate. Atmospheric Chem. Phys. 17.

Long, S.P., Ainsworth, E.A., Leakey, A.D.B., Morgan, P.B., 2005. Global food insecurity. Treatment of major food crops with elevated carbon dioxide or ozone under large-scale fully open-air conditions suggests recent models may have overestimated future yields. Philos. Trans. R. Soc. B Biol. Sci. 360, 2011–2020. https://doi.org/10.1098/rstb.2005.1749

McFadden, D., 1973. Conditional logit analysis of qualitative choice behavior.

McGrath, J.M., Betzelberger, A.M., Wang, S., Shook, E., Zhu, X.-G., Long, S.P., Ainsworth, E.A., 2015. An analysis of ozone damage to historical maize and soybean yields in the United States. Proc. Natl. Acad. Sci. 112, 14390–14395.

Mills, G., Buse, A., Gimeno, B., Bermejo, V., Holland, M., Emberson, L., Pleijel, H., 2007. A synthesis of AOT40-based response functions and critical levels of ozone for agricultural and horticultural crops. Atmos. Environ. 41, 2630–2643. https://doi.org/10.1016/j.atmosenv.2006.11.016

Mills, G., Pleijel, H., Braun, S., Büker, P., Bermejo, V., Calvo, E., Danielsson, H., Emberson, L., Fernández, I.G., Grünhage, L., Harmens, H., Hayes, F., Karlsson, P.-E., Simpson, D., 2011. New stomatal flux-based critical levels for ozone effects on vegetation. Atmos. Environ. 45, 5064–5068. https://doi.org/10.1016/j.atmosenv.2011.06.009

Mills, G., Pleijel, H., Malley, C.S., Sinha, B., Cooper, O.R., Schultz, M.G., Neufeld, H.S., Simpson, D., Sharps, K., Feng, Z., Gerosa, G., Harmens, H., Kobayashi, K., Saxena, P., Paoletti, E., Sinha, V. and Xu, X., 2018a. Tropospheric Ozone Assessment Report: Present-day tropospheric ozone distribution and trends relevant to vegetation. Elem Sci Anth, 6(1), p.47. DOI: http://doi.org/10.1525/elementa.302

Mills, G., Sharps, K., Simpson, D., Pleijel, H., Frei, M., Burkey, K., Emberson, L., Uddling, J., Broberg, M., Feng, Z., 2018b. Closing the global ozone yield gap: Quantification and cobenefits for multistress tolerance. Glob. Change Biol. 24, 4869–4893.

Mills, G., Sharps, K., Simpson, D., Pleijel, H., Broberg, M., Uddling, J., Jaramillo, F., Davies, W.J., Dentener, F., Van den Berg, M., 2018c. Ozone pollution will compromise efforts to increase global wheat production. Glob. Change Biol. 24, 3560–3574.

Monfreda, C., Ramankutty, N., Hertel, T.W., 2009. Global agricultural land use data for climate change analysis, in: Economic Analysis of Land Use in Global Climate Change Policy. Routledge, pp. 53–68.

Moore, G., Semple, J., 2009. High concentration of surface ozone observed along the Khumbu Valley Nepal April 2007. Geophys. Res. Lett. 36.

OECD, 2016. The Economic Consequences of Outdoor Air Pollution. OECD Publishing. https://doi.org/10.1787/9789264257474-en.

Osborne, S.A., Mills, G., Hayes, F., Ainsworth, E.A., Büker, P., Emberson, L., 2016. Has the sensitivity of soybean cultivars to ozone pollution increased with time? An analysis of published dose–response data. Glob. Change Biol. 22, 3097–3111.

Pleijel, H., Danielsson, H., Emberson, L., Ashmore, M., Mills, G., 2007. Ozone risk assessment for agricultural crops in Europe: Further development of stomatal flux and flux–response relationships for European wheat and potato. Atmos. Environ. 41, 3022–3040.

Reilly, J., Paltsev, S., Felzer, B., Wang, X., Kicklighter, D., Melillo, J., Prinn, R., Sarofim, M., Sokolov, A., Wang, C., 2007. Global economic effects of changes in crops, pasture, and forests due to changing climate, carbon dioxide, and ozone. Energy Policy 35, 5370–5383.

Ren, W., Tian, H., Chen, G., Liu, M., Zhang, C., Chappelka, A.H., Pan, S., 2007. Influence of ozone pollution and climate variability on net primary productivity and carbon storage in China’s grassland ecosystems from 1961 to 2000. Environ. Pollut. 149, 327–335.

Schauberger, B., Rolinski, S., Schaphoff, S., Müller, C., 2019. Global historical soybean and wheat yield loss estimates from ozone pollution considering water and temperature as modifying effects. Agric. For. Meteorol. 265, 1–15. https://doi.org/10.1016/j.agrformet.2018.11.004

Sharma, A., Ojha, N., Pozzer, A., Beig, G., Gunthe, S.S., 2019. Revisiting the crop yield loss in India attributable to ozone. Atmospheric Environ. X 1, 100008.

Shi, W., Ou, Y., Smith, S.J., Ledna, C.M., Nolte, C.G., Loughlin, D.H., 2017. Projecting state-level air pollutant emissions using an integrated assessment model: GCAM-USA. Appl. Energy 208, 511–521. https://doi.org/10.1016/j.apenergy.2017.09.122

Shindell, D., Faluvegi, G., Kasibhatla, P., Van Dingenen, R., 2019. Spatial Patterns of Crop Yield Change by Emitted Pollutant. Earths Future. https://doi.org/10.1029/2018EF001030

Shindell, D.T., 2016. Crop yield changes induced by emissions of individual climate-altering pollutants: crop yield changes per pollutant. Earths Future 4, 373–380. https://doi.org/10.1002/2016EF000377

Sicard, P., Anav, A., Marco, A.D., Paoletti, E., 2017. Projected global ground-level ozone impacts on vegetation under different emission and climate scenarios. Atmospheric Chem. Phys. 17, 12177–12196.

Singh, A.A., Agrawal, S., 2017. Tropospheric ozone pollution in India: effects on crop yield and product quality. Environ. Sci. Pollut. Res. 24, 4367–4382.

Smith, S.J., Pitcher, H., Wigley, T.M.L., 2005. Future Sulfur Dioxide Emissions. Clim. Change 73, 267–318. https://doi.org/10.1007/s10584-005-6887-y

Stohl, A., Aamaas, B., Amann, M., Baker, L.H., Bellouin, N., Berntsen, T.K., Boucher, O., Cherian, R., Collins, W., Daskalakis, N., 2015. Evaluating the climate and air quality impacts of short-lived pollutants. Atmospheric Chem. Phys. 15, 10529–10566.

Tai, A.P., Martin, M.V., Heald, C.L., 2014. Threat to future global food security from climate change and ozone air pollution. Nat. Clim. Change 4, 817.

Teixeira, E., Fischer, G., van Velthuizen, H., van Dingenen, R., Dentener, F., Mills, G., Walter, C., Ewert, F., 2011. Limited potential of crop management for mitigating surface ozone impacts on global food supply. Atmos. Environ. 45, 2569–2576.

The World Bank, The International Cryosphere Climate Initiative 2013: On Thin Ice, Washington DC. [online] Available from: https://www.worldbank.org/content/dam/Worldbank/document/SDN/Full_Repor t_On_Thin_Ice_How_Cutting_Pollution_Can_Slow_Warming_and_Save_Lives.pdf,

Thomson, A.M., Calvin, K.V., Smith, S.J., Kyle, G.P., Volke, A., Patel, P., Delgado-Arias, S., Bond-Lamberty, B., Wise, M.A., Clarke, L.E., 2011. RCP4. 5: a pathway for stabilization of radiative forcing by 2100. Clim. Change 109, 77.

Van Dingenen, R, Crippa, M., Maenhout, G., Guizzardi, D., Dentener, F., 2018a. Global trends of methane emissions and their impacts on ozone concentrations. JRC Sci. POLICY Rep.

Van Dingenen, R., Dentener, F., Crippa, M., Leitao, J., Marmer, E., Rao, S., Solazzo, E., Valentini, L., 2018b. TM5-FASST: a global atmospheric source–receptor model for rapid impact analysis of emission changes on air quality and short-lived climate pollutants. Atmos Chem Phys 18, 16173–16211. https://doi.org/10.5194/acp-18-16173-2018

Van Dingenen, R., Dentener, F.J., Raes, F., Krol, M.C., Emberson, L., Cofala, J., 2009. The global impact of ozone on agricultural crop yields under current and future air quality legislation. Atmos. Environ. 43, 604–618.

Vandyck, T., Keramidas, K., Kitous, A., Spadaro, J.V., Van Dingenen, R., Holland, M., Saveyn, B., 2018. Air quality co-benefits for human health and agriculture counterbalance costs to meet Paris Agreement pledges. Nat. Commun. 9. https://doi.org/10.1038/s41467-018-06885-9

Wang, W.-N., Cheng, T.-H., Gu, X.-F., Chen, H., Guo, H., Wang, Y., Bao, F.-W., Shi, S.-Y., Xu, B.-R., Zuo, X., 2017. Assessing spatial and temporal patterns of observed ground-level ozone in China. Sci. Rep. 7, 1–12.

Wang, X., Mauzerall, D.L., 2004. Characterizing distributions of surface ozone and its impact on grain production in China, Japan and South Korea: 1990 and 2020. Atmos. Environ. 38, 4383–4402. https://doi.org/10.1016/j.atmosenv.2004.03.067

West, J.J., Fiore, A.M., Naik, V., Horowitz, L.W., Schwarzkopf, M.D., Mauzerall, D.L., 2007. Ozone air quality and radiative forcing consequences of changes in ozone precursor emissions. Geophys. Res. Lett. 34. https://doi.org/10.1029/2006GL029173

Wise, M., Calvin, K., Kyle, P., Luckow, P., Edmonds, J., 2014. Economic and physical modeling of land use in GCAM 3.0 and an application to agricultural productivity, land, and terrestrial carbon. Clim. Change Econ. 5, 1450003.

Wu, S., Duncan, B.N., Jacob, D.J., Fiore, A.M., Wild, O., 2009. Chemical nonlinearities in relating intercontinental ozone pollution to anthropogenic emissions. Geophys. Res. Lett. 36. https://doi.org/10.1029/2008GL036607

Yi, F., Feng, J., Wang, Y., Jiang, F., 2020. Influence of surface ozone on crop yield of maize in China. J. Integr. Agric. 19, 578–589.

Young, P. J., Archibald, A. T., Bowman, K. W., Lamarque, J.-F., Naik, V., Stevenson, D. S., Tilmes, S., Voulgarakis, A., Wild, O., Bergmann, D., Cameron-Smith, P., Cionni, I., Collins, W. J., Dalsøren, S. B., Doherty, R. M., Eyring, V., Faluvegi, G., Horowitz, L. W., Josse, B., Lee, Y. H., MacKenzie, I. A., Nagashima, T., Plummer, D. A., Righi, M., Rumbold, S. T., Skeie, R. B., Shindell, D. T., Strode, S. A., Sudo, K., Szopa, S., and Zeng, G.: Pre-industrial to end 21st century projections of tropospheric ozone from the Atmospheric Chemistry and Climate Model Intercomparison Project (ACCMIP), Atmos. Chem. Phys., 13, 2063–2090, https://doi.org/10.5194/acp-13-2063-2013, 2013.

Zhao, X., Calvin, K., Wise, M., 2020. The critical role of conversion cost and comparative advantage in modeling agricultural land use change. Climate Change Economics. https://doi.org/10.1142/S2010007820500049

Zheng, B., Tong, D., Li, M., Liu, F., Hong, C., Geng, G., Li, H., Li, X., Peng, L., Qi, J., 2018. Trends in China's anthropogenic emissions since 2010 as the consequence of clean air actions. Atmospheric Chem. Phys. 18, 14095–14111.